

Thorough examination of CI engine performance metrics and emission patterns with incorporation of sustainable waste cooking oil biodiesel blends across diverse nozzle pressure regimens: A numerical study

Santosh Patel^{a,b*}, Suwarna Torgal^b & Dheerendra Vikram Singh^c

^aDepartment of Mechanical Engineering, Shri Vaishnav Institute of Technology & Science, SVVV, Indore MP 453 111, India

^bDepartment of Mechanical Engineering, Institute of Engineering & Technology, DAVV, Indore MP 452 001, India

^cNational Automotive Test Tracks (NATRAX), Dhar, MP 454 774, India

Received: 13 May 2024; accepted: 19 September 2024

Internal combustion engines consistently play a pivotal role in global transportation networks, facilitating economic growth and the interconnection of nations. Since their inception, diesel has been regarded as one of the primary fossil fuels. However, concerns about pollution and energy security drive the demand for alternative fuels. Waste cooking oil biodiesel emerges as a readily available and sustainable resource, capable of being collected and repurposed to reduce the burden on landfills and waste management systems. Using a numerical simulation tool, this study analyzes the performance and emission characteristics of a diesel engine operating on waste cooking oil. The experiments evaluate performance and emissions at various nozzle opening pressure settings, ranging from 180 to 280 bar, and compare the results with diesel. Before the experimental phase, the numerical modeling tool undergoes thorough validation against findings from previous research studies, demonstrating its ability to deliver accurate results. The study finds that blending proportions of waste cooking oil, specifically WCO10 and WCO20, yield results closest to diesel in most cases. This signifies that biodiesels with precise blending percentages can effectively address the growing need for alternative fuels.

Keywords: Waste cooking oil biodiesel, Variable nozzle pressure, Numerical simulation, CI engine, Performance, Emission

1 Introduction

Internal combustion engines have been for years an essential component of transportation networks and global mobility and since their discovery, diesel has always been considered among the primary fossil fuels. However, in the past few decades, the ever-rising transportation sector has experienced exponential growth, thus increasing fossil fuel utilization¹. Consequently, the extant dwindling in the global fossil fuel reserves and rising noxious pollutants in the earth's atmosphere clearly indicate the fallacies associated with using petroleum-based fuels, suggesting moving towards a substitute^{2,3}. In this context, biodiesel has attained worldwide importance due to its renewability and ease of production compared to conventional diesel and is being considered to cater to the potential inevitability of alternate fuel^{4,5}.

Biofuel is a sustainable and biodegradable fuel made from renewable sources like vegetable oils (e.g., soybean, canola, or palm oil) and animal fats.

Through a process called transesterification, these feedstocks are transformed into biofuel, which serves as a cleaner-burning alternative for traditional diesel fuel in diesel engines^{6,7}. As per the 2012 EASAC report, biofuel is typically categorized into three generations, primarily based on the source or origin.

First-generation biofuel is made from edible feedstocks, which include oils obtained from rapeseed, soybean, coconut, corn, palm, mustard, olive, rice, and others. The main advantages of first-generation materials are accessibility and simple processing methods. However, the key drawback is the potential impact on food supplies, leading to increased food costs⁸. Second-generation biofuel is made from inedible feedstocks such as Jatropha, Neem seed, Nagchampa, Karanja, Mahua, Rubber seed oil and others. Due to restrictions on edible feedstocks, researchers are turning to inedible feedstocks. Biofuels from the second generation provide more benefits, like being eco-friendly, cost-effective, and alleviating food resource pressure while

*Corresponding author (E-mail:santoshpatel.cad@gmail.com)

requiring less agricultural land. One of the key advantages is that it doesn't compete with food crops or valuable farmland. However, a notable drawback limited availability of plantation materials (seeds), an underdeveloped biofuel marketing system and challenge of identifying suitable land for large-scale cultivation of these feedstocks⁸⁻¹⁰. Biodiesel derived from fish oil, animal fat, microalgae, pyrolysis oil and used cooking oil are categorized as third-generation biodiesel. These viable biofuel sources overcome the issues that feedstocks from past generations had, such as economic viability, availability, food chain influence, & climate adaption. Waste frying oil is a versatile and low-cost feedstock ingredient for biodiesel manufacturing¹¹.

In 2009, the Ministry of New and Renewable Energy introduced a National Policy on Biofuels to encourage their use across the country. The amended version in 2018, implemented since May 16 of that year, set a target of blending 20% ethanol in fuel and 5% biodiesel in diesel by 2030. The primary objective of the 2018 policy is to reduce reliance on crude oil imports, increase farmers' profit, create job opportunities, utilize drylands efficiently, and encourage environmental efforts. The Prime Minister of India chairs the National Biofuel Coordination Committee and the cabinet Secretary leads the Biofuel Working Committee¹².

In our research, we utilize blends of biodiesel derived from waste cooking oil, which presents various benefits as a sustainable substitute for traditional diesel fuel. It utilizes readily available resources, reducing landfill waste and enhancing energy security by lessening dependence on imported fuels. Additionally, its production creates local job opportunities, contributing to economic growth. By adhering to the basic tenets of circular economy, it repurposes waste materials into valuable products and requires less water compared to traditional oilseed crops, aiding in water conservation. With ongoing usage of cooking oil in households and restaurants, It's a renewable feedstock for biodiesel production. Moreover, its use results in lower emissions, aligning with environmental goals to mitigate climate change and improve air quality. Governments worldwide are increasingly endorsing waste cooking oil biodiesel to meet renewable energy targets and promote circular economy initiatives, further solidifying its significance in sustainable fuel solutions¹²⁻¹⁴.

This paper comprehensively examines diesel engine performance and emission parameters by incorporating sustainable waste cooking oil biodiesel blends across

various nozzle pressure conditions using a numerical simulation tool. By systematically analyzing these variables, the research aims to provide valuable insights into the efficacy and environmental impact of utilizing waste cooking oil biodiesel blends as a renewable fuel source. The conclusions drawn from this study enrich our understanding of how biodiesel blends can enhance engine performance and mitigate emissions, providing valuable insights into their potential benefits.

2 Materials and Methods

The study systematically explores waste cooking oil (WCO) biodiesel blends as sustainable alternatives for compression ignition (CI) engines. Beginning with the collection and conversion of WCO into biodiesel via transesterification process, blends are prepared at varying concentrations (WCO10, WCO20, WCO30, and WCO100), with thorough analysis of their physicochemical properties. Engine simulation, using the validated Diesel-RK thermodynamic model, follows suit, integrating data on WCO biodiesel blends under variable nozzle pressure conditions. By inputting relevant parameters into the simulation tool based on prior research data, engine performance and emission characteristics are meticulously scrutinized and compared with conventional diesel fuel. This comprehensive assessment aims to unveil the feasibility and potential advantages of utilizing WCO biodiesel blends, offering valuable insights into sustainable energy solutions.

2.1 Biodiesel preparation and blending

Biodiesel production from waste cooking oil involves collecting used oil, filtering it with Whatman filter paper, and storing it. Transesterification reaction occurs by mixing the filtered oil with a methanol solution containing Sodium Hydroxide catalyst, preheating to 60°C, then stirring for an hour. This converts triglycerides to biodiesel and glycerol. After settling for 24 hours, glycerol is drained off. Biodiesel is washed with water, dried, and filtered to remove impurities. Blends like WCO10, WCO20, WCO30, and WCO100 (varying biodiesel-diesel ratios) are prepared^{13,15,16}. The author conducted the entire biodiesel preparation and blending process in the chemistry laboratory at SVVV, Indore. Fig. 1 shows the biodiesel preparation in SVVV chemistry lab and Fig. 2 shows the production and blending steps.

2.2 WCO Biodiesel blends properties identification

In this experiment, waste cooking oil has been utilized in four blending ratios (B10, B20, B30, and



Fig. 1 — Biodiesel preparation from waste cooking oil.

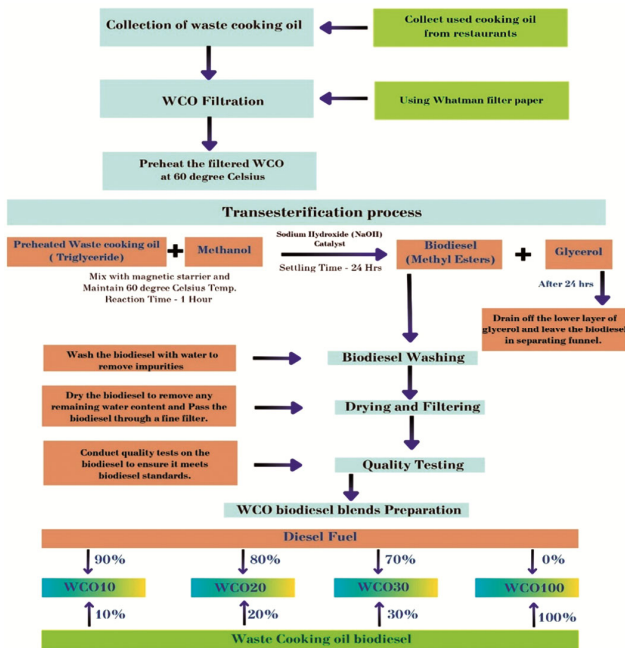


Fig. 2 — Waste cooking oil biodiesel production and blending steps.

B100) alongside pure diesel. The essential fuel properties of these biodiesel blends identified by 'Zeal Biological Testing Lab, Secunderabad, Telangana, India' are outlined in Table 1.

2.3 Experimental setup

To collect the necessary data from the engine, the engine must be properly configured Fig. 3. depicts the layout of the test engine¹⁷, which consists of a 4 - stroke, single-cylinder, CI Engine coupled to an dynamometer. The eddy current dynamometer is an instrument that determines the power imparted by a spinning shaft. Various instruments are integrated into the setup to measure various parameters including pressure, temperature, speed, fuel flow, airflow, crank angle and load. Pressure at different parts of the engine is gauged using a piezo sensor with a range of 5000 PSI. A temperature sensor with a K-type thermocouple makes it easier to detect temperatures at various engine sections. To measure the flow of water through the cooling system Rotameters are used. An AVL 444 Di gas analyzer is employed to monitor emissions, including CO, CO₂, NO_x, O₂, and unburned hydrocarbon. Additionally, an AVL-437 smoke meter is used for smokedetection¹⁸.

2.4 Simulation Work - Diesel RK Model

The Diesel-RK thermodynamic model effectively represents the working dynamics of CI engines, including energy dispersion, pressure variations, ignition delays, and engine exhaust emissions. It is specifically

Table 1 — Chemical properties of waste cooking oil biodiesel blends

Properties Name	UNIT	Waste cooking oil biodiesel blends Name					Test Method
		Diesel	WCO 10 (10 % WCO Biodiesel + 90 % diesel)	WCO 20 (20 % WCO Biodiesel + 80 % diesel)	WCO 30 (30 % WCO Biodiesel + 70 % diesel)	WCO 100 (100 % WCO Biodiesel + 0% diesel)	
Calorific Value	MJ/kg	43.286	41.684	41.301	40.738	37.114	‘ASTM D240’
Cetane Number	-	48	48.35	48.62	48.75	49.15	‘ASTM D6890’
Density at 40 °C	kg/m ³	830	834.28	840.71	846.33	884.29	‘ASTM D127’
Kinematic Viscosity at 40 °C	mm ² /s	2.542	2.753	3.084	3.301	4.915	‘ASTM D445’
Dynamic Viscosity at 40 °C	Pas.sec	0.00211	0.00229	0.00259	0.00279	0.00434	‘ASTM D445’
Carbon (C)	Mass Fraction	0.87	0.8603	0.85	0.8398	0.768	‘ASTM D5291’
Hydrogen (H)	Mass Fraction	0.126	0.1283	0.1271	0.1259	0.1174	‘ASTM D5291’
Oxygen (O)	Mass Fraction	0.004	0.0115	0.0229	0.0344	0.1146	‘ASTM D5291’
Sulphur Fraction (S)	%	0.002	0.0019	0.0018	0.0017	0.001	‘ASTM D6667’

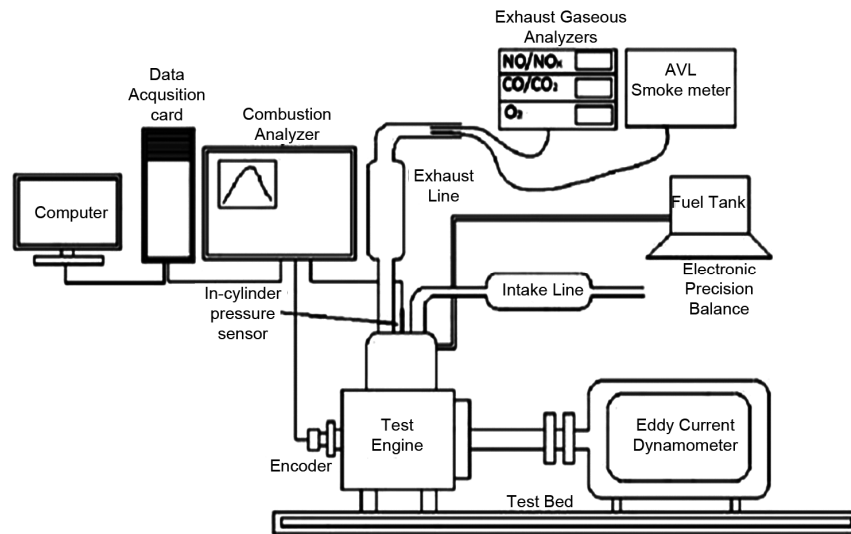


Fig. 3 — Schematic Layout of test engine.

designed for CI engine simulations and multi-parameter optimization. Diesel RK offers a versatile platform for simulating various engine configurations, ensuring comprehensive performance analysis under different conditions. It provides a cost-effective and time-efficient alternative to costly experimental setups, allowing for quick exploration of the impact of variables like Nozzle pressure, valve timings and compression ratio. With efficient parametric sensitivity analysis, researchers can assess engine performance and emissions parameter frequently to input changes, it provides while the ease of model iteration facilitates the exploration of a wider range of scenarios¹⁹⁻²².

Considering these factors helps us better understand why Diesel RK is a great option for engine analysis in

specific research or practical applications. Even though there have been many studies using different biofuels with both numerical and experimental methods, the Diesel-RK Model shines as a practical and viable tool. This is especially true when compared to commercially available Computational Fluid Dynamics (CFD) software, which usually require higher costs and longer computation times¹⁹⁻²². The all-necessary steps of Diesel-RK Model shown in Fig 4.

2.4.1 Numerical Method - Governing equation for Diesel-RK model

The Diesel-RK modeling tool applied to this research employs an account of a set of equations including mass and energy conservation, friction, heat, and NOx

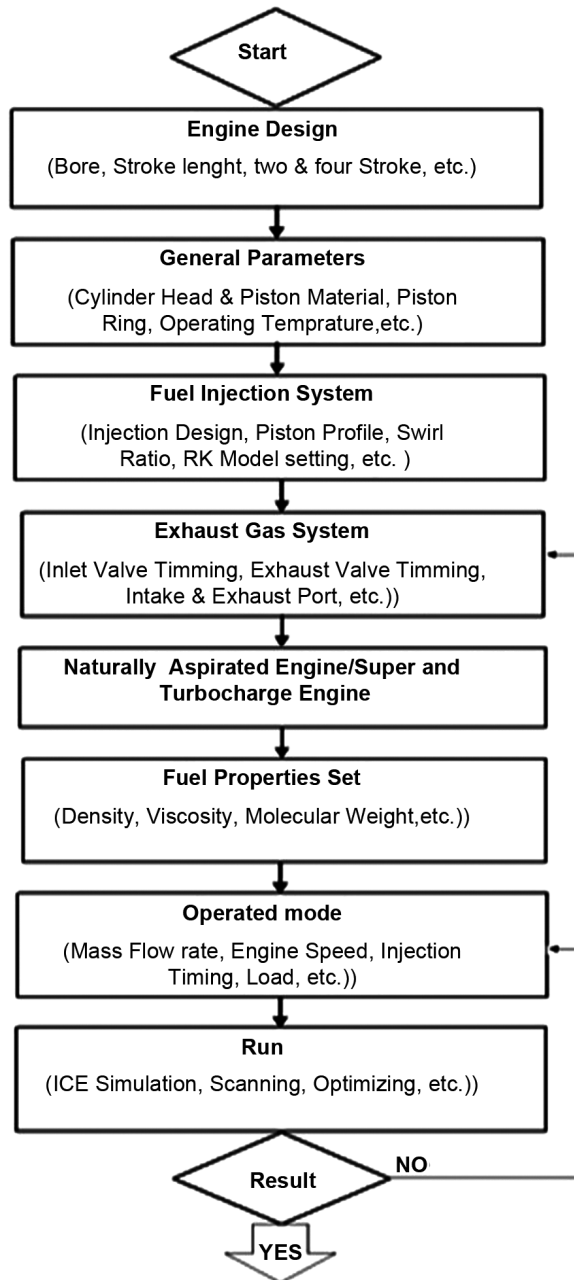


Fig. 4 — Steps of Diesel-RK Model.

models. It applies the law of conservation of energy to assess an internal combustion engine's performance potential, combustion traits, and environmental impact. The Tool has numerous zones separated into seven phases for computing combustion outcomes and relies on the Zeldovich mechanism for computing NO_x emissions. Table 2 and Table 3 outlines the mathematical equations (1 – 15) governed by the numerical model^{23–30}, while Table 4 contains the equations (16 – 25) for the performance parameters^{31,32}.

2.5 Tool validation

The primary focus of this study was to assess the operational performance and emissions behavior of a CI engine using different proportions of WCO biodiesel blends. To achieve this objective, the authors opted to utilize the numerical tool Diesel-RK, which effectively provided the results for the various biodiesel blends tested^{33,34}. To corroborate the results generated by the numerical tool, the authors undertook a validation procedure for the tool. This involved replicating the experimental setup and operating conditions from a previously conducted experimental study Gnanasekaran *et al.*¹⁸ and applied these replicated conditions to the simulation tool and results were compared to ascertain the accuracy of the Diesel-RK tool's predictions. Table 5 Provides breakdown of the input engine parameters used during the tool validations¹⁸. These validations were carried out at 100% engine load with diesel as the primary fuel. The findings from the examination are displayed in graphical representation (Fig. 5 – Fig. 10) and as well as in tabular format Table 6.

The validation results show errors ranging from 1.74% to 6.44%. Most errors are below 4%, with only one case showing a maximum error of around 7%. From these findings, it is evident that the Numerical tool Diesel-RK is validated for subsequent exploration.

2.6 Engine specification for current study

Our research focuses on examining the impact of various WCO biodiesel blends on the performance behavior and emission attributes of an CI engine across a range of nozzle pressure conditions, spanning from 180 to 280 bar. Following the analysis of the results, all findings are compared with diesel to assess feasibility. Initially, trials were carried out at a standard speed of 1500 rpm, 17.5 CR, Ambient pressure 1 bar, Temp. 288 K, Fuel injection initiates 23⁰ bTDC, Top clearance 1 mm and 100 % loading conditions.

The parameters pertaining to fuel injection are summarized in Table 7, whereas Table 8 provides the specifications for the test engines²⁴.

3 Results and Discussion

In this investigation, the Performance metrics and exhaust emission constituents' results were calculated at different nozzle pressure values. These values were kept at an interval of 20 bars, and the results were found on 180, 200, 220, 240, 260, and 280 bar, respectively.

Table 2 — Numerical model Diesel-RK governing equations²³⁻²⁶

Equation Name	Governing equation
Mass Conservation	$\frac{dm}{dt} = \sum_j \dot{m}_j$ (1)
i^{th} species gross generation rate	$\dot{s}_{gen} = \nu W_m \Omega_i$ (2)
Equations for Species	$\frac{d(m_i Y)}{dt} = \sum_j Y_i^j \dot{m}_j + \dot{s}_{gen}$ (3)
Species conservation equation	$\dot{Y}_i = \sum_j \left(\frac{\dot{m}_j}{m}\right) (Y_i^j - Y_i^{cyl}) + \frac{W_m \Omega_i}{\rho}$ (4)
Conservation of energy	$\frac{d(mu)}{dt} = -p \frac{dv}{dt} + \frac{dQ_{ht}}{dt} + \sum_j \dot{m}_j$ (5)
where, m = total mass (in kg) m_i = Mass of the i^{th} species \dot{m}_j = Mass generation rate of the j^{th} species (kg/s) $\frac{dm}{dt}$ = rate of change of mass (within any open system) \dot{s}_{gen} = i^{th} species net generation rate (kg/s) W_m = weight (kg/mol.) ν = specific volume (kg/m ³) Y_i = mass fraction ρ = density (kg/m ³)	
Heat Release during ignition delay	$\tau = 3.8 \times 10^{-6} (1 - 1.6 \times 10^{-4} \cdot n) \sqrt{\frac{T}{p}} \exp\left(\frac{E_a}{8.312T} - \frac{70}{25+CN}\right)$ (6)
Heat release rate during controlled combustion	$\frac{dx}{d\tau} = \Phi_0 \times \left(A_0 \left(\frac{m_f}{v_i}\right) \times (0.1 \times \sigma_{ud} + x_0) \times (\sigma_{ud} - x_0)\right) + \Phi_1 \times \left(\frac{d\sigma_u}{d\tau}\right)$ (7)
Combustion heat generation rate	$\frac{dx}{d\tau} = \Phi_1 \times \left(\frac{d\sigma_u}{d\tau}\right) + \Phi_2 \times \left(A_2 \left(\frac{m_f}{v_c}\right) \times (\alpha - x) \times (\sigma_u - x)\right)$ (8)
Heat release rate during late combustion phase	$\frac{dx}{d\tau} = (\alpha \xi_b - x) \times (1 - x) \times \Phi_3 A_3 K_T$ (9)
where, τ = Time in second P = pressure (MPa) E_a = Energy of activation CN = Cetane number n = Speed of Engine T = Temperature (K) P = Pressure (bar) $\Phi_0 = \Phi_1 = \Phi_2 = \Phi_3$ = Constant (which describes the completeness of fuel vapor combustion in the zones. K_T = Evaporation constant x_0 = Burnt fuel fraction during the delay period $\frac{dx}{d\tau}$ = Rate of heat generation (1/s.) $A_0 = A_1 = A_2 = A_2$ = empirical factor ξ_b = efficiency (air use) α = equivalence ratio (air and fuel) σ_u = Fraction of fuel evaporated current σ_{ud} = Fraction of fuel evaporated current	

Table 3 — Governing equations for emissions²⁷⁻³⁰

Equation Name	Governing equation
Zeldovich Mechanism	$O_2 \rightleftharpoons 2O$ (10)
	$N_2 + O \rightleftharpoons N + NO$ (11)
	$N + O_2 \rightleftharpoons O + NO$ (12)
NO concentration during Combustion phase	$\frac{d[NO]}{d\theta} = \frac{2.333 \times 10^{-7} \cdot P \cdot e^{-\frac{38020}{T_b}} [O]_e [N_2]_e \left\{1 - \left(\frac{[NO]}{[NO]_e}\right)^2\right\}}{T_b \cdot R \cdot \left(1 + \frac{2365}{T_b} \left[\frac{[NO]}{[O_2]_e}\right] e^{-\frac{2365}{T_b}}\right)} \times \frac{1}{\omega}$ (13)

(Contd.)

Table 3 — Governing equations for emissions^{27–30}

Equation Name	Governing equation
Soot formation	Smoke(Hartridge) = $100[1 - 0.9545e^{(-2.4226[C])}]$ (14)
Hartridge smoke level	$\left(\frac{d[C]}{dt}\right)_K = 0.004 \frac{q_c dx}{V dt}$ (15)

where,

NO = Nitric oxide

O₂ = Oxygen

ω = Angular velocity (rpm)

R = Constant

q_c = Cycle fuel mass (kg)

V = Rate of current volume

$\frac{dx}{dt}$ = Rate of heat release (J/s)

Table 4 — Performance indicators equations^{31,32}

Performance Indicators	Mathematical expressions
Supply of heat	$Q_{in} = m_f Q_{HV} \eta_c$ (16)
Steady-state heat supply	$\dot{Q}_{in} = \dot{m}_f Q_{HV} \eta_c$ (17)
Available engine energy	$\dot{W} = \dot{m}_f Q_{HV}$ (18)
Brake thermal efficiency	$(\eta_t)_{brake} = \dot{W}_b / \dot{m}_f Q_{HV} \eta_c$ (19)
Indicated thermal efficiency	$(\eta_t)_{ind} = \dot{W}_i / \dot{m}_f Q_{HV} \eta_c$ (20)
Mechanical efficiency	$\eta_m = \dot{W}_b / \dot{W}_i$ (21)
Volumetric efficiency	$\eta_v = V_a / V_d$ (22)
Torque	$\tau = F \times r$ (23)
Brake Mean effective pressure	$BMEP = 2\pi n \tau / V_d = (\tau \times L_s) / (V_s \times K)$ (24)
Brake Specific Fuel Consumption	$BSFC = \dot{m}_f / BP$ (25)

where,

Q_{in} = Heat Supplied

Q_{HV} = Calorific value of fuel

η_c = fuel conversion efficiency

m_f = mass of fuel for one cycle

\dot{m}_f = Mass flow rate of fuel

\dot{W}_b = BP = Brake power

\dot{W}_i = IP = Indicated Power

V_a = Actual volume of air intake

V_d = Displacement volume

τ = Brake torque

n = engine speed in RPM

L_s = Stroke Length

V_s = Swept volume

K = number of cylinders

3.1 Brake power

Its sometimes-called piston engine power, signifies the power developed at the engine crankshaft throughout the engine's working cycle³⁵. In this numerical study, the brake power (kW) values were derived at varying nozzle pressure levels. The average BP of the WCO biodiesel blends WCO10, WCO20, WCO30 and WCO100 respectively, were found 3.68%, 3.80%, 6.30%, and 8.32% lower than diesel.

Moreover, the conclusive numerical study on different waste cooking oil blends has displayed that the minimum percentage difference between the rake power values of diesel and WCO10 was calculated as 3.50% (lower than diesel) at a nozzle pressure of 240 bar. Similarly, the minimum percentage difference of WCO20, WCO30, and WCO100 from diesel, were determined as 3.89%, 3.59%, and 7.08% at the nozzle pressure values of 200, 260, and 260 bar,

Table 5 — Tool validation input details

Engine Parameters	Tool Validation
Operating fuel	Diesel
Cooling type	Air cooled
Rated output power	4.4 kW
Cylinder volume	661 cc
Engine CR	17.5:1
Bore	87.5 mm
Stroke	110 mm
Combustion clearance	36.87 cc
Injection start timing	24 °bTDC
Injection pressure	180 bar
Operating load and speed	Full-load, 1500 rpm

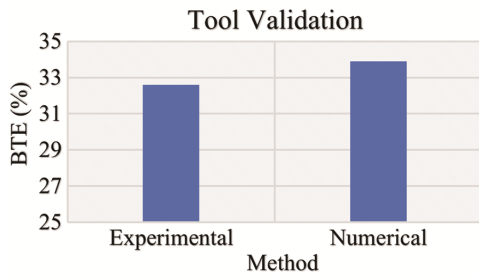


Fig.5 — Brake thermal efficiency comparison by experimental & numerical method.

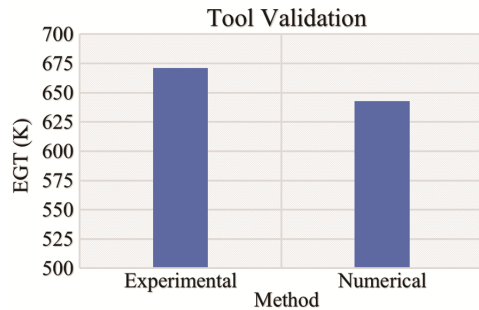


Fig. 6 — Exhaust gas temperature comparison by experimental & numerical method.

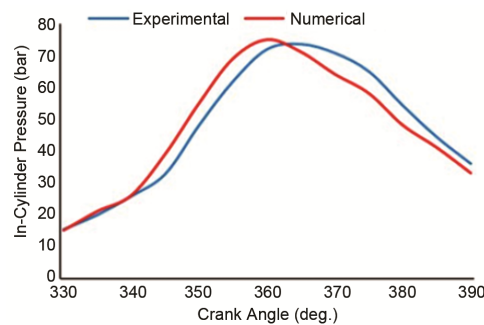


Fig. 7 — In-cylinder pressure analysis by experimental & numerical method.

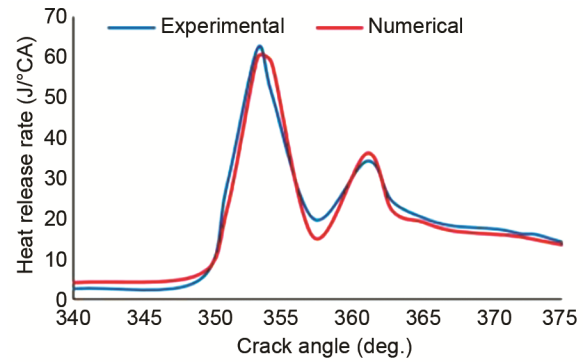


Fig. 8 — Heat release rate analysis by experimental & numerical method.

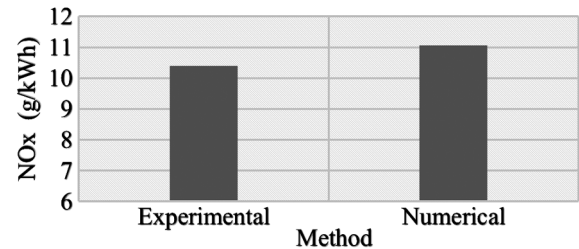


Fig. 9 — NO_x emission analysis by experimental & numerical method.

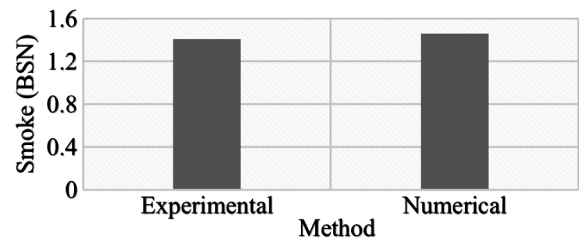


Fig. 10 — Smoke emission analysis by experimental & numerical method.

respectively. All the numerical values are nearest to the given nozzle pressure. The numerical study indicates an increment in brake power as the nozzle pressure increases. The highest brake power was found at 280 bar of nozzle pressure for all blends, as indicated in Fig. 11.

3.2 Brake torque

After eliminating significant losses such as frictional and pumping losses, the net value of torque transferred by the crankshaft to the transmission system is often known as the brake torque³⁶. In this assessment, the brake torque (kW) values were derived at varying nozzle pressure settings. These values were kept at an interval of 20 bars, and the results were found on 180, 200, 220, 240, 260 and

Table 6 — Outcomes of tool validation at full load condition

Tool Validation	Test characteristics					
	BTE (%)	EGT (K)	CPP (bar)	HRR (J/deg)	NO _x (g/kWh)	Smoke (BSN)
Experimental Method (Gnanasekaran <i>et al.</i> ¹⁸)	32.6	671.15	73.6	62	10.4	1.41
Present Work - Numerical Method Results	33.89	642.93	74.88	59.9	11.07	1.46
Error (%)	3.95	4.20	1.74	3.38	6.44	3.54

Table 7 — Engine nozzle details

Parameter	Value
Period of injection	29 ⁰ CA
Injection start timing	23 ⁰ b TDC
Nozzle quantity	3
Max injection pressure	180 – 280 bar (Variable Range)
Orifice injector nozzle bore	0.22 mm
A/F ratio	1.75
Spray offset from bowl axis	2.5 mm
Atmospheric temperature	288 K
Atmospheric pressure	1 bar
Loading condition	100%

Table 8 — Engine details

Indicators	Values
Engine category	Single cylinder, 4 Stroke
Engine type	CI Engine
Cooling system	Water cooling system
Engine CR	17.5
Engine RPM	1500 rpm
Method of Lubricating	Forced lubrication
Length of connecting arm	235 mm
Piston travel	110 mm
Clearance at TDC	1 mm
Cylinder dia.	80 mm
Head architecture	Dual-valve setup
Piston alloy	Aluminum alloy
Cylinder alloy	Aluminum alloy
Piston shape	Bowl geometry
liner thickness	5.6 mm
Average liner temp. (at TDC)	400 K
Inlet tract length	160 mm
Inlet tract dia.	38.1 mm
Outlet tract length	160 mm
Outlet tract diameter	34 mm

280 bar, respectively. The average BT of the WCO blends B10, B20, B30, and B100 respectively, were found 3.68%, 3.80%, 6.30%, and 8.32% lower than diesel. Moreover, the conclusive numerical study on different waste cooking oil biodiesel blends has displayed that the minimum percentage difference between the brake torque values of diesel and WCO10 was calculated as 3.50% (lower than diesel) at a nozzle pressure of 240 bar. Similarly, the brake

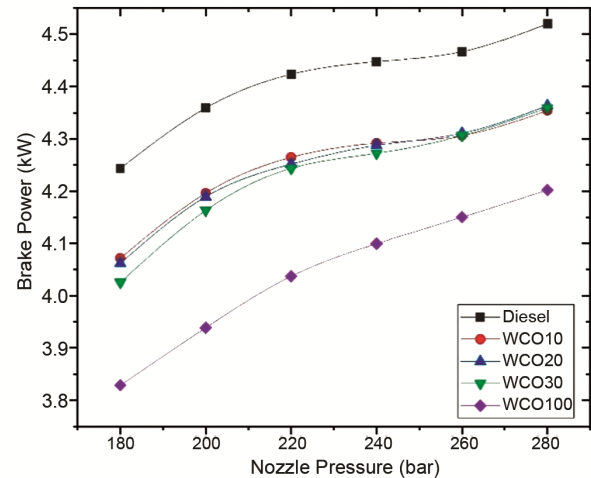


Fig. 11 — Brake power analysis of WCO blends at different nozzle pressure values.

torque values for WCO20, WCO30 and WCO100 are lower than diesel by 3.89%, 3.59%, and 7.08% and were closest to it at the nozzle pressure values of 200, 260, and 260 bar, respectively. The conclusive study suggests that as the pressure of the fuel sprayed by the nozzle increases, the brake torque also increases. The highest brake torque was found at 280 bar of nozzle pressure for all WCO blends. The blends which were nearby to the diesel values were WCO10, WCO20, and WCO30, as illustrated in Fig. 12.

3.3 Indicated efficiency

Indicated efficiency, on the other hand, quantifies the ratio of energy within indicated power to fuel-provided power¹⁹. In this numerical study, the average IE of WCO10 biodiesel blend is 0.18% higher than diesel and in case of blends WCO20, WCO30 and WCO100 the average indicated efficiency are 0.49%, 2.95% and 7.48% lower than diesel. Moreover, the conclusive numerical study on different waste cooking oil biodiesel blends has displayed that the maximum percentage difference between the indicated efficiency values of diesel and WCO10 was calculated as 0.25% (farest value - higher than diesel)

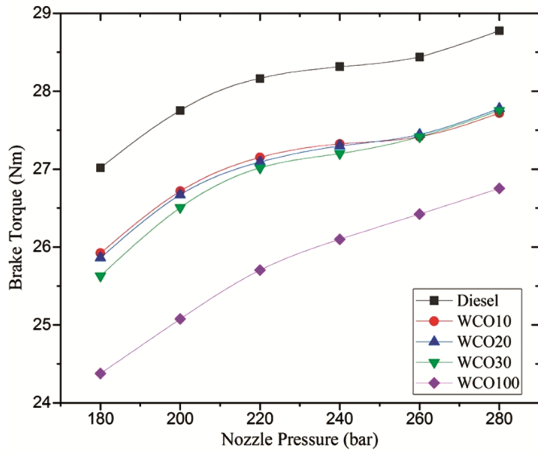


Fig. 12 — Brake torque analysis of WCO blends at different nozzle pressure values.

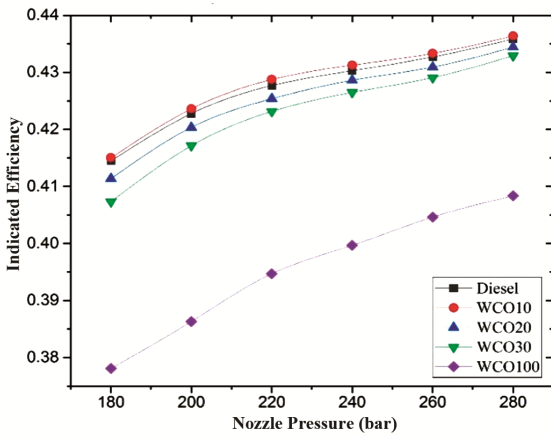


Fig. 13 — Indicated efficiency analysis of WCO blends at different nozzle pressure values.

at a nozzle pressure of 220 bar. Similarly, the indicated efficiency values for WCO20, WCO30, and WCO100, are lower than diesel by 0.32%, 0.67% and 6.30% and were closest to it at the nozzle pressure value of 280 bar. The conclusive study displays that as the nozzle pressure was increased, the indicated efficiency was also increased. The highest indicated efficiency was found at 280 bar nozzle pressure for all WCO blends. The WCO blends with indicated efficiency near the diesel values were found B10, B20, and B30, with B10 being the closest to the diesel. However, the WCO10 blend surpassed the diesel in terms of indicated efficiency at all nozzle pressure settings, as depicted in Fig. 13.

3.4 Brake mean effective pressure

It signifies the mean pressure to exerted to the engine's pistons, that would be required to generate the measured brake horsepower output³⁷.

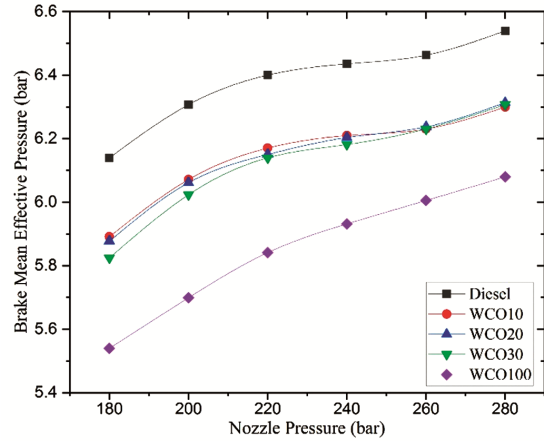


Fig. 14 — Brake mean effective pressure analysis of WCO blends at different nozzle pressure values.

In this numerical method, the average BMEP values for the WCO biodiesel blends WCO10, WCO20, WCO30 and WCO100, respectively, were found 3.68%, 3.80%, 6.30% and 8.32% lower than diesel. Moreover, the conclusive research on different waste cooking oil blends has displayed that the minimum percentage difference between the BMEP value of diesel and WCO10 was calculated as 3.50% (lower than diesel) at the nozzle pressure of 240 bar. Similarly, BMEP for WCO20, WCO30, and WCO100 are lower than diesel by 3.89%, 3.59%, and 7.08% and closest to it at the nozzle pressure 200, 240, and 260 bar, respectively. The research demonstrates an increase in BMEP with rising nozzle pressure. The highest values of BMEP were found at 280 bar of nozzle pressure for all WCO blends and the blends WCO10, WCO20, and WCO30 are found nearer to diesel in terms of 'break means effective pressure' values, as indicated in Fig. 14.

3.5 Specific fuel consumption

SFC indicate the amount of fuel consumed by the engine to generate a unit of power over a specific period³⁸. In this numerical study, the average SFC readings for the WCO10, WCO20, WCO30 and WCO100 blends were found to be 4.45%, 6.14%, 9.59% and 27.20% higher compared to diesel. Furthermore, the conclusive investigation into different WCO biodiesel blends has shown that, under a nozzle pressure of 240 bar, the least percentage variation in SFC values between diesel and WCO10 was computed as 4.33% greater than diesel. Likewise, the SFC outcomes for WCO20, WCO30, and WCO100 blends exceeded that of diesel by 5.88%, 3.45%, and 25.32%, respectively, with their values

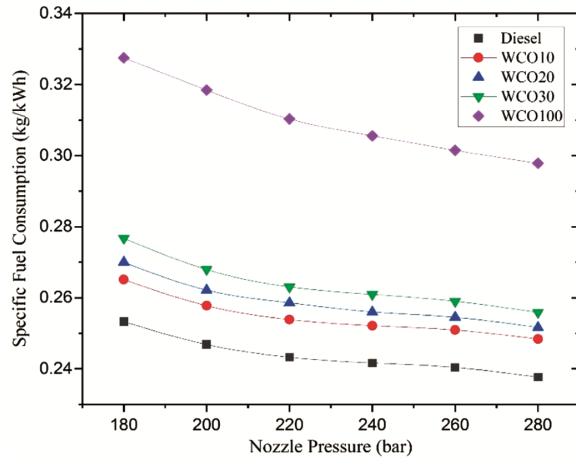


Fig. 15 — Brake specific fuel consumption analysis of WCO blends at different nozzle pressure values.

converging closest to diesel at a nozzle pressure of 280 bar. The conclusive investigation reveals a reduction in brake-specific fuel consumption with increasing nozzle pressure. The minimum specific fuel consumption value was observed at a nozzle pressure of 180 bar for all waste cooking oil biodiesel blends, as depicted in Fig 15.

3.6 CO₂ emission

The carbon dioxide produced by internal combustion engines is a result of the combustion of atmospheric oxygen with the carbon present in the operating fuel³⁹. In this numerical study, the average CO₂ emission of the blends WCO10, WCO20, WCO30 and WCO100 respectively, were found 3.29%, 3.70%, 7.01% and 12.29% higher than diesel. Moreover, the conclusive numerical study on different waste cooking oil biodiesel blends has displayed that the minimum percentage difference between the CO₂ Emission values of diesel and WCO10 was calculated as 3.17% (higher than diesel) at a nozzle pressure of 240 bar. Similarly, the CO₂ emission values for WCO20, WCO30 and WCO100 are higher than diesel by 3.45%, 3.92% and 10.63% and were closest to it at the nozzle pressure of 200, 280, and 280 bar, respectively. The conclusive study suggests a decay in the CO₂ emission as the pressure of the fuel sprayed by the nozzle increases. The highest value of CO₂ emission was found at 180 bar of nozzle pressure and the lowest at 280 bar of nozzle pressure for all WCO blends, as depicted in Fig. 16.

3.7 SO₂ emission

The atmospheric air combines with the sulfur present in the fuel to result in sulfur dioxide. If this

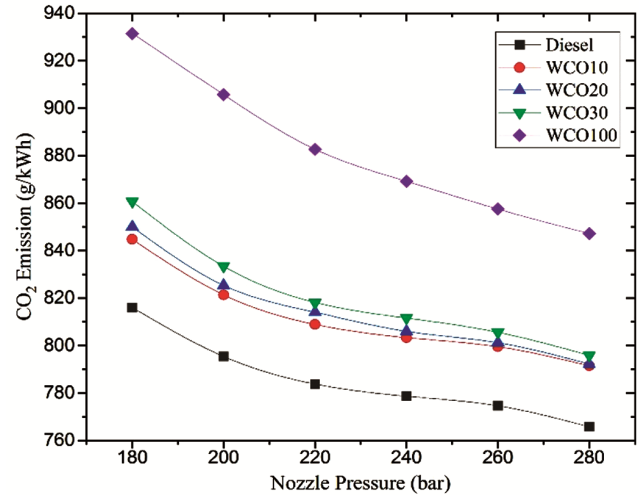


Fig. 16 — Carbon dioxide emission analysis of WCO blends at different nozzle pressure values.

resultant further reacts with oxygen, sulfur trioxide is obtained, which is highly toxic in nature⁴⁰.

In this numerical study, Across the WCO10, WCO20, WCO30, and WCO100 blends, the mean SO₂ emissions were calculated to be 1.74%, 5.41%, 7.98% and 31.01% lower than diesel, respectively. Moreover, the conclusive numerical study on different waste cooking oil biodiesel blends has displayed that the maximum percentage difference between the SO₂ Emission values of diesel and WCO100 was calculated as 38.93% (farest value - lower than diesel) at a nozzle pressure of 280 bar. Similarly, the SO₂ emission values for WCO10, WCO20 and WCO30 are lower than diesel by 3.27%, 7.17% and 10.86% and were farest to it at the nozzle pressure value of 280 bar for all blends. The study indicates that as the nozzle pressure increases, the SO₂ emission decreases. The peak SO₂ emission occurred at a nozzle pressure of 180 bar, while the minimum was observed at 280 bar for all blends. and the pure biodiesel blend WCO100 emitted the minimum SO₂ emission compared to all other blends and diesel also, as illustrated in Fig. 17.

3.8 NO_x emission

NO_x emissions, including NO and NO₂, arise from engine combustion, triggered by the engine's high temperatures and pressures interacting with nitrogen and oxygen in the surrounding air⁴¹⁻⁴³. The average NO_x emission for WCO10, WCO20, WCO30, and WCO100 blends, respectively, were 13.63%, 8.48%, 7.70% and 8.65% lower than diesel. Moreover, the conclusive numerical study on different waste

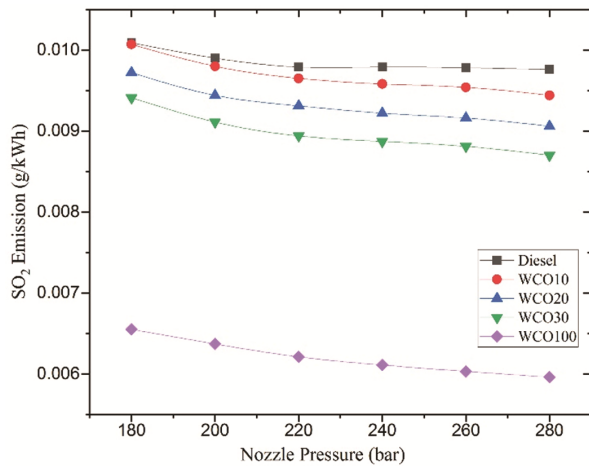


Fig.17 — Sulphur dioxide emission analysis of WCO blends at different nozzle pressure values.

cooking oil biodiesel blends has displayed that the maximum percentage difference between the NO_x emission values of diesel and WCO10 was calculated as 15.33% (lower than diesel) at a nozzle pressure value of 280 bar. Similarly, the NO_x emission values for blends WCO20, WCO30, and WCO100 are lower than diesel by 10.83%, 6.80% and 9.80% and were found farrest to it at the nozzle pressure of 280, 260, and 280 bar, respectively. The conclusive study indicates nozzle pressure was increased; the NO_x concentration was also increased. The highest NO_x in exhaust gas was found at 260 bar of nozzle pressure for all WCO blends. The WCO30 blend is nearby to the diesel in terms of NO_x concentration. The NO_x emission value decreases as the nozzle pressure increases till 200 bar. However, further increment in nozzle pressure (to 260 bar) results in an increased NO_x emission, and then NO_x emission also decreases when pressure increases to 280 bar, as indicated in Fig. 18.

3.9 PM emission

The formation of particulate matter often occurs as a result of combustion, where air combines with fuel residues. These particles typically comprise soluble organic fractions and dry spots⁴⁴.

The study's numerical findings indicate that PM emissions for WCO10, WCO20, WCO30, and WCO100 blends are, on average, 2.60%, 15.52%, 52.32% and 175.43% higher than those of diesel, respectively. Moreover, the conclusive numerical study on different waste cooking oil biodiesel blends has displayed that the minimum percentage difference between the PM emission values of diesel and

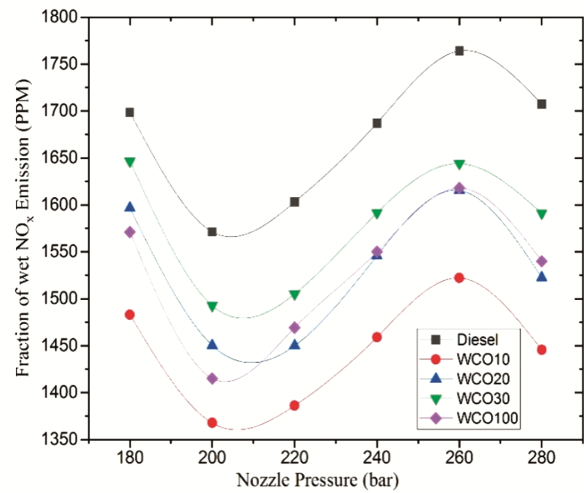


Fig. 18 — Wet NO_x fraction analysis of WCO blends at different nozzle pressure values.

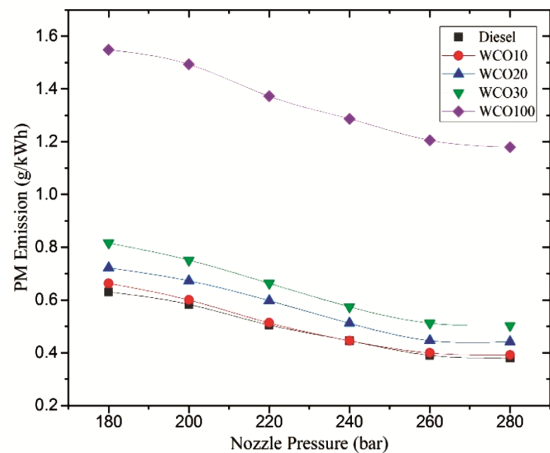


Fig.19 — Particulate matter emission analysis of WCO blends at different nozzle pressure values.

WCO10 was calculated as 0.067% (lower than diesel) at a nozzle pressure of 240 bar. Similarly, the PM emission values for blends WCO20, WCO30 and WCO100 are higher than diesel by 14.15%, 31.17%, and 209.87% and were closest to it at the nozzle pressure of 260, 260 and 280 bar, respectively. The ultimate findings indicate that as nozzle pressure rises, there's a decline in PM emissions. The study revealed that the highest PM emission occurred at a nozzle pressure of 180 bar, while the lowest was observed at 280 bar for all blends. Among the blends, WCO10 closely resembles diesel in terms of PM emission values, as depicted in Fig. 19.

4 Conclusion

Analyzing the performance metrics and emission patterns of a diesel engine using waste cooking oil

biodiesel blends at various nozzle pressure settings using numerical techniques yielded several conclusions. The data reveals a progressive increase in brake power, brake torque, indicated efficiency, indicated mean effective pressure, and brake mean effective pressure as the nozzle opening pressure is raised. Conversely, SFC, CO₂ emission, SO₂ emission, and particulate matter values showed a gradual decline with increasing nozzle pressure. However, Fluctuations in NO_x emission values were observed with the incremental increase in nozzle pressure.

In the instance of the WCO10 blend, the most favorable operating parameters were achieved within the range of 260 to 280 bar nozzle pressure, resulting in the highest levels for brake power, brake torque, brake mean effective pressure, indicated efficiency, and the minimal specific fuel consumption. The WCO10 blend has also delivered optimal results in emissions, providing the lowest NO_x, CO₂, PM and SO₂ emissions compared to other blends. Overall, this blend has provided optimal results while testing the performance and emission properties, even surpassing diesel in a few of the aforementioned characteristics. Similarly, the WCO20 and WCO30 blends demonstrated satisfactory performance across different nozzle pressure values, with notable improvements in emissions such as SO₂ and NO_x. Conversely, the WCO100 blend exhibited lower SO₂ emissions at higher nozzle pressures, emphasizing the need for careful selection of nozzle pressure for each blend to achieve optimal engine performance and emission control.

In conclusion, the thorough exploration of engine performance metrics and emissions pattern under varying nozzle pressure conditions emphasizes the intricate correlations between fuel constituents, engine architecture and operational factors. Further investigation into optimizing nozzle pressure alongside engine design is crucial to fully harnessing the potential of WCO blends as sustainable alternatives to diesel fuel. Moreover, exploring advanced combustion technologies and emission control strategies tailored specifically to WCO blends can play a pivotal role in realizing cleaner and more efficient diesel engines, paving the way towards a greener future.

Acknowledgment

The authors would like to thank Dr. S. Venkatesan Jayakumar, an Associate Professor in the Chemistry Department at Shri Vaishnav Institute of Science, for his invaluable support in preparing waste cooking oil

biodiesel in the chemistry laboratory. Additionally, they express gratitude to Dr. Shrikant Pandey, the Head of the Mechanical Engineering Department at SVITS, SVVV, Indore, for facilitating access to the laboratory facilities required for the research.

References

- Demirbas A, Bafail A, Ahmad W & Sheikh M, *Energy Explor and Exploit*,34 (2016) 290.
- Jhalani A, Sharma D, Soni S L, Sharma P K & Sharma S, *Env Sci Pol and Res*,26 (2019) 4570.
- Saydut A, Erdogan S, Kafadar A B, Kaya C, Aydin F & Hamamci C, *Fuel*, 183 (2016) 512.
- Shahir S A, Masjuki H H, Kalam M A, Imran A, Fattah I M R &Sanjid A, *Ren and Sust Ener Rev*, 32 (2014) 379.
- Ghadikolaei M A, Cheung C S & Yung K F, *Fuel*, 235 (2019) 288.
- Subramaniam D, Murugesan A, Avinash A &Kumaravel A, *Ren and Sust Ener Rev*, 22 (2013) 361.
- Ahmad M, Practical Handbook on Biodiesel Production and Properties,(CRC Press Florida, USA) ISBN: 978-1-4665-0744-9, 2012, p. 1.
- Singh D, Sharma D, Soni S L, Sharma S,Sharma P K& Jhalani A, *Fuel*, 262(2020)116553.
- Suresh M, Jawahar C P & Richard A, *Ren and Sust Ener Rev*, 92 (2018) 38.
- Atabani A E, Silitonga A S, Ong H C, Mahlia T M I, Masjuki H H & Badruddin I A, *Ren and Sust Ener Rev*, 18 (2013) 211.
- Shameer P M & Ramesh K, *Energy*, 118 (2017) 1334.
- Das S. *NPB India: A Persp Ener Poli*, 143 (2020) 111595.
- de Araújo C D M, de Andrade C C, de Silva E D S &Dupas F A, *Renew and Sust Ener Rev*, 27 (2013) 445.
- Shirneshan A, *Proc Social and Behav Sci*, 75 (2013) 292.
- Marchetti J M, Miguel V U &Errazu A F, *Ren and SustEner Rev*, 11(2007) 1300.
- Encinar J M, González J F & Rodríguez-Reinares A, *Fuel Proc Tech*, 88 (2007) 513.
- Uyumaz A, *Fuel*, 267 (2020) 117150.
- Gnanasekaran S, Saravanan N &Ilangkumaran M, *Energy*,116 (2016) 1218.
- Rajak U, Nashine P, Singh T S & Verma T N, *Energy Conv and Mgmt*, 156 (2018) 235.
- Rajak U & Verma T N, *Energy Conv and Mgmt*, 180 (2019) 904.
- Krishania N, Rajak U, Chaurasiya P K, Singh T S, Birru A K & Verma T N, *Fuel*, 276 (2020) 118123.
- Rajak U, Nashine P & Verma T N, *Fuel*, 262 (2020) 116519.
- Fiveland S B & Assanis D N, *SAE Transactions:Journ of engines*, 109 (2000) 452.
- Patel S, Torgal S, Purohit T, Kumar R, Singh D V, Kanchan S, Soudagar M E M , Ahamad T , Kalam M A and Patel M, *Pro Inst of Mech Eng, Part E: J Pro Mech Eng*, (2023) 09544089231190221.
- Kuleshov A S, *SAE Tech Paper*, (2005) 2119.
- Kuleshov A S, *SAE Tech Papers*, (2006) 1385.
- Datta A & Mandal B K, *Energy*, 125 (2017) 470.
- Lavole G A, Heywood JB & Keck J C, *Comb Sci and Tech*, 1(1970) 313.
- Petranović Z, Vujanović M & Duić N, *J Clean Prod*, 88 (2015) 272.

- 30 Alkidas A C, *SAE Tech Paper*, (1984) 840412.
- 31 Pulkrabek W W, *Engineering Fundamentals of the Internal Combustion Engine*, (Pearson New Inter Ed, Edinburgh Gate, Harlow London), 2ndEdn, ISBN:978-1-269-37450-7, 2014, p. 41.
- 32 Heywood J B, *Internal Combustion Engine Fundamental*, (Mc Graw Hill Edu New York, United states) 2ndEdn, ISBN: 978-1-26-011611-3, 2018, p. 121.
- 33 Datta A & Mandal B K, *Appl ThermEng*, 98 (2016) 670.
- 34 Wakode V R & Kanase-Patil A B, *Appl ThermEng*, 113 (2017) 322.
- 35 Çetinkaya M, Ulusoy Y, Tekin Y & Karaosmanoğlu F, *Ener Conv Mgt*, 46 (2005) 1279.
- 36 Wang S, Zhu X, Somers L M T & de Goey L P H, *Ener Conv Mgt*, 149 (2017) 918.
- 37 Islam M A, Rahman M M, Heimann K, Nabi M N, Ristovski Z D, Dowell A, Thomas G, Feng B, Von A N & Brown R J, *Fuel*, 143 (2015) 351.
- 38 Senthur Prabu S, Asokan M A, Roy R, Francis S & Sreelekh M K, *Energy*, 122 (2017) 638.
- 39 Lanjekar R D & Deshmukh D. *Rene and Sust Ener Rev*, 54 (2016) 1401.
- 40 Rajak U, Nashine P & Verma T N, *ARPJ Eng and Appl Sci*, 5(2018) 1.
- 41 Uslu S & Celik M B, *Fuel*, 262 (2020) 116496.
- 42 Simsek S & Uslu S, *Fuel*, 279 (2020) 118528.
- 43 Li Y, Jia M, Chang Y, Xie M & Reitz R D, *Energy*, 99 (2016) 69.
- 44 Wang J, Wu F, Xiao J & Shuai S, *Fuel*, 88(2009) 2037.